# Numerical simulation of the dynamic behaviour of a degraded insulated rail joint

Yang, Z; Boogaard, MA; Li, Z; Dollevoet, RPBJ

**DOI**
10.4203/ccp.110.240

**Publication date**
2016

**Document Version**
Accepted author manuscript

**Published in**
Proceedings of the 3rd international conference on railway technology: Research, development and maintenance

Paper 0123456789

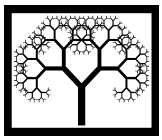


Proceedings of the Third International Conference on Railway Technology: Research, Development and Maintenance, J. Pombo, (Editor),
Civil-Comp Press, Stirlingshire, Scotland.

# Numerical Simulation of the Dynamic Behaviour of a Degraded Insulated Rail Joint

**Z. Yang, M.A. Boogaard, Z. Li and R.P.B.J. Dollevoet**
**Section of Railway Engineering**
**Delft University of Technology**
**The Netherlands**

## Abstract

Due to the significant discontinuity in stiffness and geometry, the insulated rail joint (IRJ) is considered as one of the weakest parts in the track structure. The wheel-rail impact over a joint may lead to track deterioration and increased maintenance costs. The impact load is believed to be closely associated with the dynamic behaviour of track and conditions of track components at the joint section. In this paper, the dynamic behaviour of a typical IRJ in the Dutch railway network is studied numerically. A three dimensional finite element (FE) IRJ model is set up and an explicit time integration scheme is employed to simulate a hammer test conducted on the IRJ. The simulated frequency response functions (FRFs) of the IRJ are then calculated and some typical resonant behaviours can be deducted. Based on the numerical model, the influence of various deterioration types on the dynamic behaviours of IRJ are predicted under the controlled conditions.

**Keywords:** insulated rail joint, hammer test, accelerance, finite element method, track deterioration.

## 1 Introduction

The insulated rail joints (IRJs) have been widely used in the railway network for many years, as they can separate track circuits. However, due to the significant discontinuity in stiffness and geometry, the joint is considered as one of the weakest parts in the track structure. When a train runs over an IRJ, wheel-rail impact inevitably happens and may lead to track deterioration and increased maintenance costs. Since the wheel-rail impact load is believed to be closely associated with the dynamic behaviour of track and conditions of track components at the IRJ section, a better understanding of the dynamic behaviour of IRJ and the influence of malfunction of track components may provide an insight into a sustainable IRJ design and a more efficient track maintenance.

Because of its infinite nature, the dynamic behaviour of track structure is more often characterised by the frequency response functions (FRFs) rather than the characteristic modes [1]. Hammer test is a widespread method for the identification of the FRFs of track structures [2-4], but its specific application to the IRJ is limited. Recently, a systematic hammer measurement was performed on IRJ by Oregui et. al [5] to assess the health condition of IRJs; the dynamic behaviour in the vertical direction was studied. A small number of samples cannot represent the changes of dynamic behaviour of the track deterioration types.

Compared to field measurement, a reliable modelling work can investigate the influential factors of IRJ dynamic behaviour under controlled conditions and then attribute the change of dynamic behaviour to certain track deterioration type. The IRJ can be modelled either analytically or numerically. Considering the bending stiffness at the joint is dramatically reduced, the IRJ was often simplified as a pin or spring in the analytical models, when the structural complexity could be neglected [6-7]. When it comes to the study of the high-frequency contact-impact behaviour or component failure, a more complex numerical model would be required [8-9]. Since both the high frequency responses up to 5 kHz and the influences of track component conditions are desired in this study, a three dimensional finite element (FE) model is established and a hammer test is simulated with an explicit time integration scheme. Finally, a parameter variation is conducted to investigate how the dynamic response can be affected by degraded IRJs.

# 2 Finite element (FE) model

In order to obtain a better understanding of the influential factors on dynamic behaviour of the IRJ under controlled conditions, a finite element (FE) model is developed and an explicit time integration scheme is applied to simulate the hammer test carried out at IRJ. The IRJ model together with the excitation/response positions of the hammer test simulated is explained in this section.

## 2.1 IRJ model

The three dimensional FE IRJ model shown in Fig. 1 is developed from the track model presented in [10]. The IRJ, including 2 fishplates, 4 pairs of bolts and a 6 mm gap, is modelled in the middle of a 10 meter half-track. The rail is UIC54 with an inclination of 1:40. The fastenings are modelled with spring/damper elements. The two neighbouring timber sleepers (yellow) beneath the IRJ have baseplate fastenings and the concrete sleepers (red) elsewhere are with Vossloh fastenings. These two fastening types are differentiated by spring/damper parameters. Bolts are simplified as 4 pairs of opposite loads, pressing the fishplates onto the web of the rails. Compared to the model in [10], the sleepers and fishplates have realistic geometries and reduced mesh size in this study. In addition, the lateral dynamics can be considered more accurately in this improved model by including the lateral stiffness and damping in the fastening models.

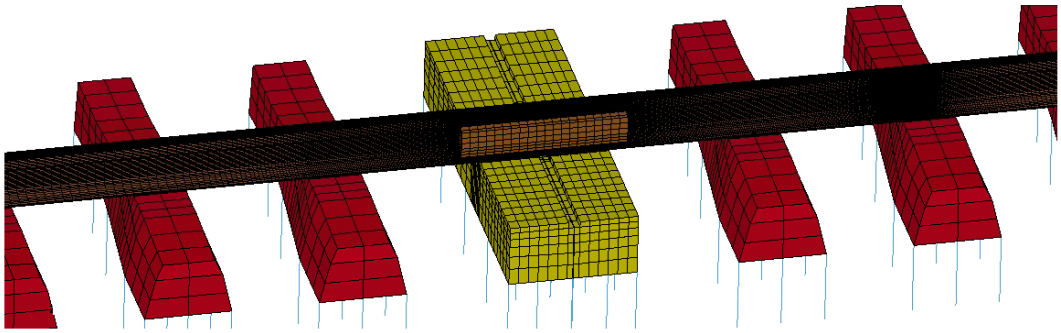

Figure 1: FE IRJ model

## 2.2 Excitation/response positions

An explicit time integration method is then applied to simulate a hammer test. The hammer impulse excitation is represented by a triangular function as [11]. Since the dynamic behaviour under the wheel-IRJ impact is of most concern, the hammer excitation in this work is exerted just after the joint along the train travel direction, and normally onto the rail top surface, as shown in Fig. 2. The vertical and lateral responses are recorded at three sections after the joint, respectively rail-end, on-support and mid-span, where different dynamic features can be expected. The measurement points of these three sections are denoted by numbers 1-6 in Fig. 2. In addition, the vertical dynamic responses of the rail-end and on-support sections before the joint, denoted by numbers 7-8, are also recorded in order to investigate the vibration transmission across the joint.

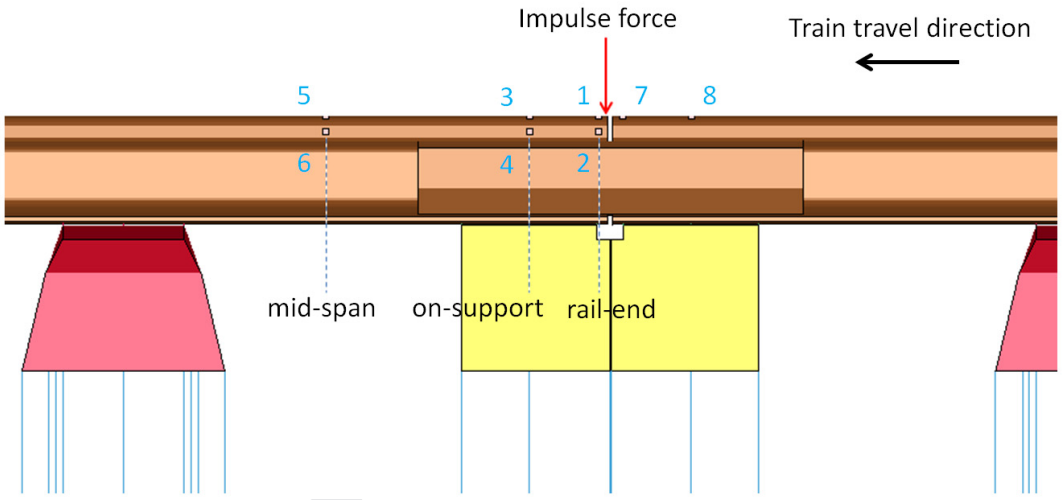


Figure 2: Schematic diagram of excitation/response positions in the FE IRJ model (White squares with blue numbers denote the response positions; red arrow indicates the excitation positions)

# 3 Simulated dynamic responses of the FE model

## 3.1 Time-domain vibration response

The time-domain vibration response is analysed by comparing the simulated time histories of accelerations at the 8 testing points depicted in Fig. 3.

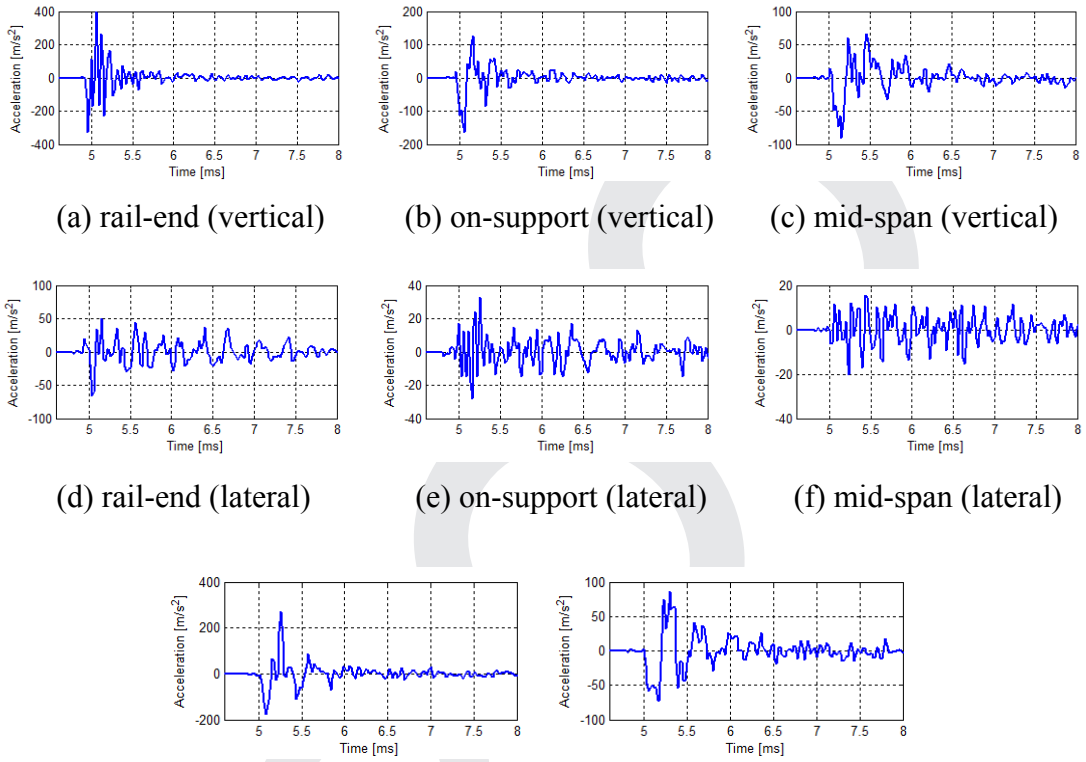


(a) rail-end (vertical) (b) on-support (vertical) (c) mid-span (vertical)

(d) rail-end (lateral) (e) on-support (lateral) (f) mid-span (lateral)

(g) rail-end-other side (vertical) (h) on-support-other side (vertical)

Figure 3: Time histories of acceleration responses at the IRJ

It can be seen that all the time histories show an impulse response pattern: the signal starts with a peak and decays gradually with certain exponential rate. The maximum acceleration reaches up to 400 m/s$^2$ and happens in the vertical response of rail-end section, closest to the excitation point. The signals are damped in both the vertical direction (from (a) to (c)) and the lateral direction ((d) to (f)) with the increase in the distance to the excitation point. Although the amplitudes of the vertical accelerations are higher than those of lateral ones, they are damped much faster. That's because the excitation was exerted vertically and the vertical damping of track system is substantially higher than the lateral one. Due to the energy dissipation during the transmission to the other side of joint, the acceleration amplitudes at the corresponding testing points on the other side of joint are relatively low ((a) to (g), and (b) to (h)).

## 3.2 Point accelerance

Since the vibration response of IRJ model is recorded by the acceleration, the accelerance is applied in this paper to characterise its dynamic behaviour. The simulated point accelerances of the three testing sections after IRJ are depicted in Fig. 4 (a) and (b), respectively, for vertical and lateral directions. From Fig. 4 (a), some typical vertical resonant behaviours of track can be found: the pinned-pinned resonance occurs at about 1 kHz, where peaks are found in the accelerances of rail-end and mid-span and a dip in that of on-support. In addition, the broad peaks at about 280 Hz and the dips at about 450 Hz in all the three curves can respectively correspond to the '$f_2$ resonance' of the rail mass on the fastening stiffness and the '$f_a$ anti-resonance' where the sleepers vibrate on the ballast and pad stiffness, according to [12]. Finally, The anti-resonance at about 2.5 kHz is attributed to the 2$^{nd}$ order pinned-pinned resonance, which is close to that of a track without the IRJ measured in [4]. The general level of the lateral cross point accelerances shown in Fig. 4 (b) is much lower than the vertical ones in (a). Over 2 kHz, the lateral response of rail-end is evidently higher than the other two sections, presenting a high frequency dynamic feature, possibly related to the less vibrating mass at the rail-end.

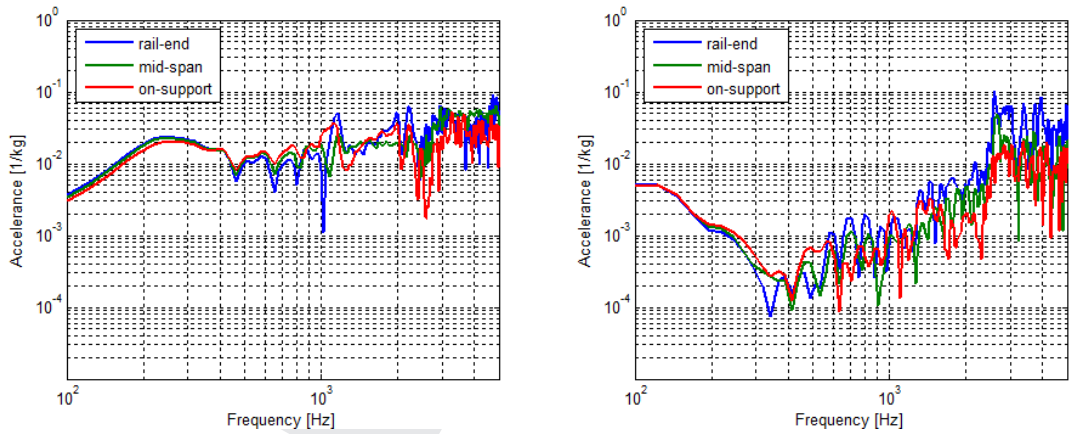


(a) vertical (b) lateral

Figure 4: Point accelerances after the IRJ

By comparing the point accelerances of the two sides of the IRJ in Fig. 5, we can see that the main difference occurs at the frequency range over 2 kHz. As concluded in [1], the low-frequency (below 2 kHz) dynamic behaviour of rail can be represented by a simple beam; while the rail cross-section deformation plays important roles in its dynamics over 2 kHz. Therefore, it can be deduced that, under the simulated excitation, the cross-section deformations experienced by the rail model at the two sides of a joint are different but their beam-like dynamic behaviours can be in close proximity.

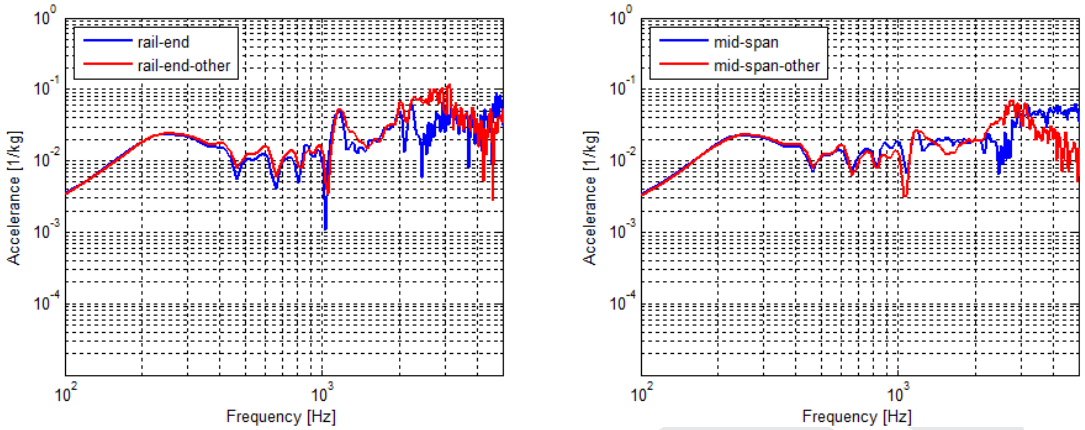


(a) section of rail-end (b) section of mid-span

Figure 5: Comparison of the dynamic behaviours of two sides of IRJ

# 4 Responses of the damaged IRJs

The parameter variation is performed in this section. The FE model aforementioned is taken as the reference to investigate how the dynamic response of the IRJ may change when significant deteriorations arise.

## 4.1 Fastening failure

The dynamic response of the IRJ with fastening failure is simulated by setting the stiffness and damping of the baseplate fastenings to zero. By comparing the power spectral densities (PSDs) at three sections of the deteriorated IRJ with the reference (Fig. 6), it can be seen that the $f_2$ resonance is intensified. That is because the baseplate fastenings have great influence on the vibration absorbing and transmitting at this frequency. The failed fastenings may also damp the high frequency responses over the 2nd order pinned-pinned resonance at rail-end and on-support sections to some extent. This can be due to the reason that the great deformations of rail cross-section close to the joint are decreased when releasing the fastenings.

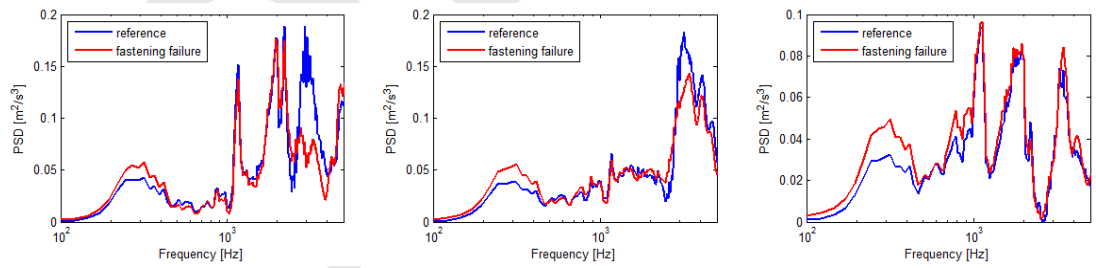


(a) rail-end (position 1) (b) on-support (position 3) (c) mid-span(position 5)

Figure 6: Comparison of PSDs of accelerations of the reference IRJ (blue) and the deteriorated IRJ with failed fastenings (red)

## 4.2 Voided sleeper

Voided sleeper is simulated by setting the stiffness and damping of the ballast beneath two the timber sleepers to zero, so that the timber sleepers can be considered suspended under the IRJ by the baseplate fastenings. In this case, the rail vibrations at all the three sections are damped at around 280 Hz ( $f_2$ resonance) and 3 kHz ($2^{nd}$ order pinned-pinned resonance), as shown in Fig. 7 (a)-(c); while the vibration of timber sleeper is amplified mainly below 280 Hz ( $f_2$ resonance) and at 450 Hz ($f_a$ resonance), see in Fig. 7 (d).

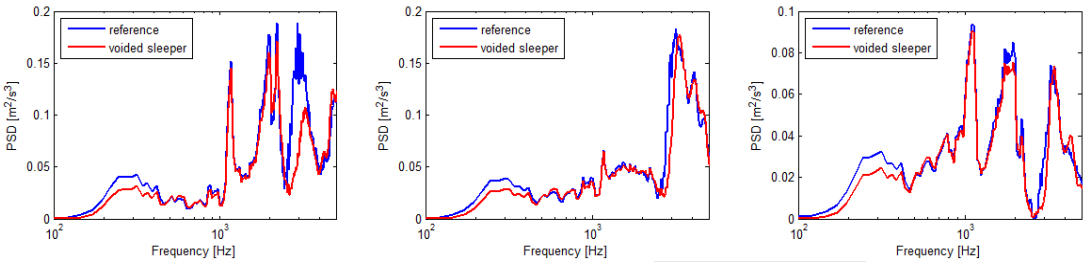


(a) rail-end (position 1) (b) on-support (position 3) (c) mid-span(position 5)

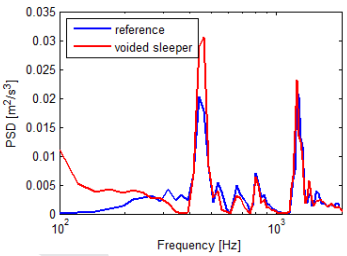


(d) timber sleeper

Figure 7: Comparison of PSDs of accelerations of the reference IRJ (blue) and the deteriorated IRJ with voided sleepers (red)

## 4.3 Bolt looseness

The joint connection, including the tightness of bolts and the healthy condition of fishplates, can significantly influence the vibration transmission from one side of joint to the other. Therefore, the dynamic responses of both sides of the IRJ are analysed in Section 4.3 (Bolt looseness) and Section 4.4 (broken fishplates).

Since bolts are simplified as 4 pairs of opposite loads in the model, the bolt looseness can be simulated by, e.g., removing the last pair of loads along the traffic direction. Affected by the bolt looseness, the PSDs of the responses after the IRJ, shown in 8 (a) and (b), increase in the frequency range higher than the pinned-pinned resonance but less energy are transmitted through the loose joint connection to the other side of joint, shown in Fig. 8 (c) and (d).

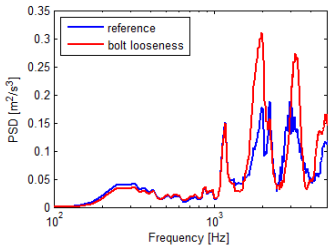


(a) rail-end after IRJ (position 1)

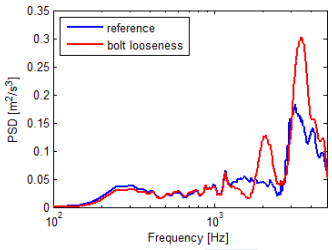


(b) on-support after IRJ (position 3)

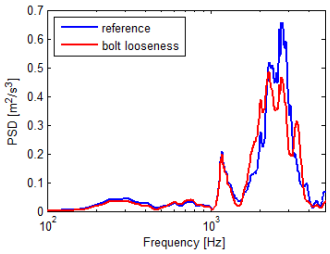


(c) rail-end before IRJ (position 7)

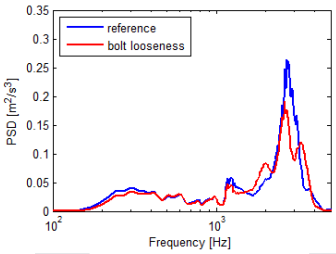


(d) on-support before IRJ (position 8)

Figure 8: Comparison of PSDs of accelerations of the reference IRJ (blue) and the deteriorated IRJ with a loose bolt (red)

## 4.4 Broken fishplates

Broken fishplates are simulated by reducing the elastic modulus of the fishplates to 1% of that in the reference condition. The results shown in Fig.9. indicates that, due to the change of the constrain condition at the rail end, the vibration response of the rail under the excitation will be dramatically increased (Fig. 9 (a) and (b)) over the whole frequency range; while only a small part of the low-frequency vibration energy can be transferred to the other side of the IRJ (Fig. 9 (c) and (d)).

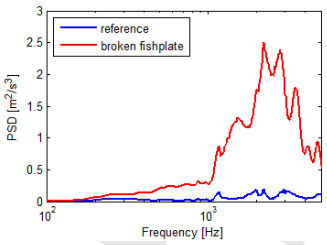


(a) rail-end-after (position 1)

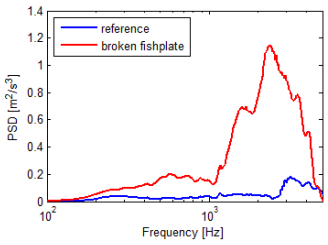


(b) on-support-after (position 3)

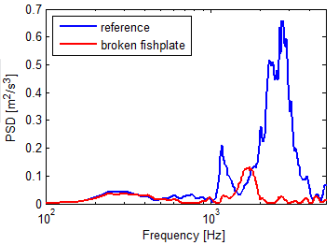


(c) rail-end-before (position 7)

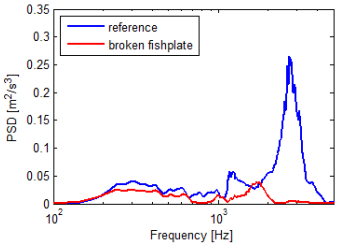


(d) on-support-before (position 8)

Figure 9: Comparison of PSDs of accelerations of the reference IRJ (blue) and the deteriorated IRJ with broken fishplates (red)

# 5 Conclusions and future work

In this paper, an explicit time integration finite element method is employed to study the dynamic behaviours of IRJ numerically. The simulated typical track resonances of the $f_2$, $f_a$, the 1st and 2nd order pinned-pinned are respectively around 280 Hz, 450 Hz, 1 kHz and 2.8 kHz. The influence of the various deterioration types on the dynamic behaviours of IRJ are analysed with the model and some conclusions are drawn: fastening failure and voided sleeper have great influences on the $f_2$ resonance and the frequency responses over the 2nd order pinned-pinned resonance. The bolt looseness mainly affects the frequency responses higher than the pinned-pinned resonance. Broken fishplates can isolate the vast majority of high-frequency vibration from the other side of joint.

The IRJ model presented in this paper will be validated in future work by comparing with a field measurement. The dynamic wheel-IRJ interaction model will then be established for investigating the impact loads and vibrations of IRJs of different dynamic behaviours, which may contribute to optimised and sustainable IRJ designs.

# References


[1] D.J. Thompson.: Railway Noise and Vibration : Mechanisms, Modelling and Means of Control. Elsevier, 2009.

[2] D.J. Thompson, N. Vincent, "Track dynamic behaviour at high frequencies, part 1: theoretical models and laboratory measurements", Vehicle System Dynamics, 24, 86-99, 1995.

[3] A.P. De Man, "A survey of dynamic railway track properties and their quality", PhD thesis, Delft University of Technology, 2002.

[4] M. Oregui, Z. Li, R. Dollevoet, "Identification of characteristic frequencies of damaged railway tracks using field hammer test measurements", Mechanical Systems and Signal Processing, 54, 224-241, 2015.

[5] M. Oregui, M. Molodova, R. Dollevoet, Z. Li, "Experimental investigation into the condition of insulated rail joints by impact excitation", Experimental Mechanics, 55, 1597-1612, 2015.

[6] T.X. Wu, D.J. Thompson, "On the impact noise generation due to a wheel passing over rail joints", Journal of Sound and Vibration, 267, 485-496, 2003.

[7] T. Kitagawa, K. Murata, T. Kawaguchi, S. Tanaka, K. Nagakura, "Experimental and theoretical studies on impact noise generation due to rail joints", Notes on Numerical Fluid Mechanics and Multidisciplinary, 126, 55-62, 2015.

[8] Z. Wen, X. Jin, W. Zhang, "Contact-impact stress analysis of rail joint region using the dynamic finite element method", Wear, 258, 1301-1309, 2005.

[9] A.K. Himebaugh, R.H. Plaut, D.A. Dillard, "Finite element analysis of bounded insulated rail joints", International Journal of Adhesion & Adhesives, 28, 142-150, 2008.

[10] Z. Yang, Z. Li, S. Rahimi, R.P.B.J. Dollevoet, "Numerical simulation of impact noise generated at the railway insulated joint", ISMA2014, Leuven, Belgium, 2014.
[11] M. Oregui, Z. Li, R. Dollevoet, "An investigation into the vertical dynamics of tracks with monoblock sleepers with a 3D finite-element model", Journal of Rail and Rapid Transit, DOI: 10.1177/0954409715569558.
[12] N. Vincent, D.J. Thompson, "Track dynamic behaviour at high frequencies, part 2: Experimental results and comparisons with theory", Vehicle System Dynamics, 24, 100-114, 1995.